*Journal of Scientific Exploration,* Vol. 25, No. 4, pp. 735–746, 2011 0892-3310/11

RESEARCH

# Color Distribution of Light Balls in Hessdalen Lights Phenomenon

**Gerson S. Paiva**
*gerson_trabalho@yahoo.com.br*

**Carlton A. Taft**
*gcatff@terra.com.br*

*Centro Brasileiro de pesquisas Físicas, Rua Dr. Xavier Sigaud, 150*
*22290-180, Rio de Janeiro, Rio de Janeiro, Brazil*

Submitted 9/6/2011; Accepted 10/7/2011

**Abstract**—Hessdalen lights (HL) are unexplained light balls usually seen in the valley of Hessdalen, Norway. In this work, we present a model to explain the spatial color distribution of luminous balls commonly observed in HL phenomenon. According to our model, these light balls are produced by electrons accelerated by electric fields during rapid fracture of piezoelectric rocks under the ground. Semi-relativistic light balls in the HL phenomenon are produced by ionic acoustic waves (IAW) interacting with a central white-colored light ball of HL phenomenon.

*Keywords*: Hessdalen Lights—Rock piezoelectricity—electron avalanche—Fractoemission

## Introduction

Several rare and unexplained light phenomena can be seen in the atmosphere. For example, ball lightning (Paiva, Pavão, Vasconcelos, Mendes, & Silva, 2007), blue jets (Pasko & George, 2002), red sprites (Pasko, Inan, & Bell, 2000), and terrestrial gamma ray flashes (TGFs) (Paiva, Pavão, & Bastos, 2009, Paiva, 2009). Hessdalen Lights (HL) are unexplained lights usually seen in the valley of Hessdalen, Norway (Teodorani, 2004). They have the appearance of a free-floating light ball with dimensions ranging from decimeters up to 30 m. HL often show strong pulsating magnetic perturbation of about 5 Hz. They are often accompanied by small, short-duration pulsating "spikes" in the HF and

VLF radio ranges, sometimes showing Doppler features. HL explicitly shows visually some kind of “satellite spheres” around a central luminous core. The absolute luminosity of this cluster of light balls has been estimated to be about 19 kW. The empirical evidence is that the small balls which can be ejected to a large distance (on the order of 50–100 m) from the large white-colored nucleus tend to be green-colored, while the small balls that appear to be very close (distance on the order of 2–5 m) to a cluster nucleus tend to be white- (high intensity) or red- (high intensity) and blue- (low-intensity) colored.

The reason for the different colors, which are apparently related to distance from the nuclear region, remains unknown (Teodorani, 2004). According to Teodorani (2004), the production of balls of distinctly different color, recorded at Hessdalen, differs from standard ball lightning behavior. If so, then the color of the light balls might be produced by quantum dots from mold spores on just one side of the plasma or by natural aerosols whose nature varies with locality. Quantum dots are nanoparticles made from a semiconducting material and range in diameter from 2–10 nm. Spontaneous production of almost mono-disperse quantum dots might come from mold spores, as the main semi-conducting elements, decomposed by the central plasma of the light ball. However, this theory does not explain the color intensity of satellite light balls.

No existing theory or model can account for all (and sometimes contradictory) observations of HL. One explanation attributes the phenomenon to an incompletely understood combustion process in air involving clouds of dust from the valley floor containing scandium (Bjorn, 2007). Some sightings, though, have been identified as misperceptions of astronomical bodies, aircraft, car headlights, and mirages (Leone, 2003).

A theory that has attracted great attention was proposed by Takaki and Ikeya (1998). It involves piezoelectricity generated under a rock strain. Change in seismic stress releases piezo-compensating, bound charges due to changes in the piezoelectric polarization of quartz grains in granitic rocks, which produces an intense electric field at the fault zone. In the specific Hessdalen area, where light phenomena are seen very often some meters over the ground, an electric triggering mechanism above might be produced by the existing high abundance of quartz, copper, and iron underground. When quartz is subjected to tectonic stress, it generates piezoelectricity (Lockner, Johnston, & Byerlee, 1983), while copper is an ideal electricity conductor and consequently might be an electrical amplifier of the HL phenomenon.

One recent hypothesis suggests that the lights are formed by a cluster of macroscopic Coulomb crystals in a plasma produced by the ionization of air and dust by alpha particles during radon decay in the dusty atmosphere (Paiva

& Taft, 2010). Coulomb crystal is a regular structure (cubic, triangular, etc.) formed by microparticles (dust) in the plasma of electrons and ions under certain conditions. Several physical properties (oscillation, geometric structure, and light spectrum) observed in Hessdalen Lights phenomenon can be explained through the dust plasma model.

Enomoto and Hashimoto (1990) have detected the emission of charged particles from indentation fracture of rocks. The charge generated by hornblende andesite indentation fracture is about $1.2 \times 10^{-11}$ C/s. The volume of the fractured zone, estimated from the size of the indent, was $0.02 \times 10^{-9}$ m$^3$. Thus, the net production rate would be ~0.6 C/m$^3$/s. If a massive fracture occurs during one second at ground level, over an area extending some meters, the charge generated may be compared to the total electric charge produced by one bolt of lightning (1 Coulomb). Charge separation on fractured surfaces produces high electric fields on the order of $10^6$–$10^7$ V cm$^{-1}$, causing the field emission of electrons in the atmosphere. The energy of emitted electrons may be in the keV range. This may be sufficient to cause geoelectromagnetic disturbances.

Ogawa, Oike, and Miura (1985) showed in laboratory experiments that rocks radiated wide-band EM waves (10 Hz–100 kHz) when they were struck by a hammer and fractured. Very low frequency EM emission (0.01–10 Hz) was also observed from earth rocks before and during earthquakes according to Park, Johnson, Madden, Morgan, and Morrison (1993). Satellites showed intense EM radiation at frequencies below 450 Hz (Serebryakova, Bilichenko, Chmyrev, Parrot, Rauch, Lefeuvre, & Pokhotelov, 1992). These data are in accord with the EM signals recorded by the spectrum analyzer and the magnetometer at Hessdalen covering the band of 0.5–80 MHz (Strand, 1990). So it appears that EM waves could have been emitted by rocks in the region where strange lights were observed.

In this work, we present a model to explain the spatial color distribution of luminous balls commonly observed in HL phenomenon. According to our model, different colors of light balls in HL phenomenon are produced by accelerated electrons due to electric fields formed by rapid fractures of piezoelectric rocks under the ground during water freezing (i.e. during the winter). Semi-relativistic green light balls in the HL phenomenon are produced by the light emission of ionic oxygen transported by ionic acoustic waves (IAW) interacting with a large white-colored light ball of HL phenomenon.

## The Model

Let us consider the model of the HL cluster shown in Figure 1.

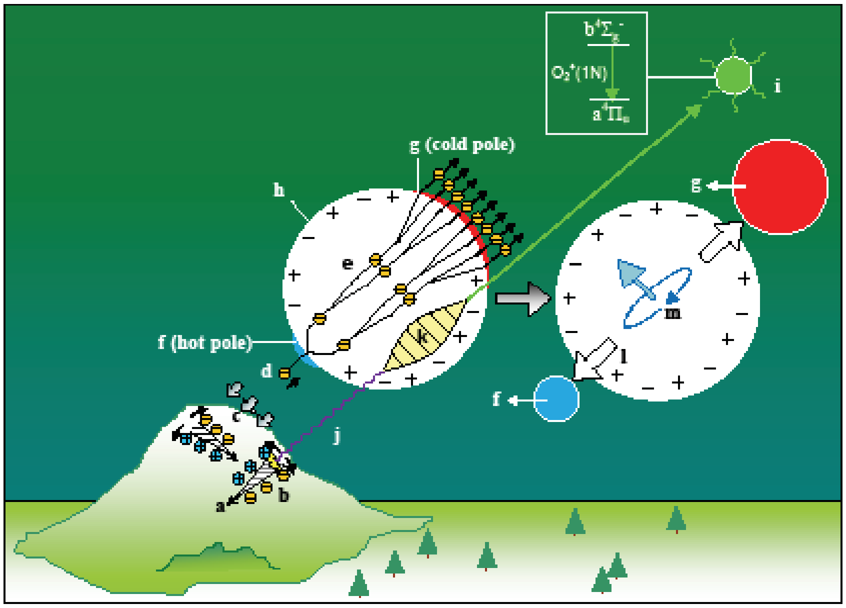


**Figure 1. Light balls in HL cluster: Rock fractures under the hill ground (a), charge separation (b), high electric fields (c), acceleration of these electrons in the atmosphere (d), electron-avalanche (e), low-intensity blue-colored light ball (f), high-intensity red-colored light ball (g), central white-colored light ball (h), small green light ball (i), very low frequency electromagnetic waves (j), ion-acoustic waves (k). Rotation (l) of the central white ball (m) ejecting its hot and cold edges, forming, respectively, blue (f) and red light balls (g).**

According to Figure 1, the abrupt rock fractures under the hill ground (a) (probably produced by water expansion during freezing in the lithosphere) results, temporarily, in charge separation (b). One possibility is that charge separation on fractured surfaces produces high electric fields on the order of $10^6$–$10^7$ V cm$^{-1}$ (c). Free electrons with the density of $4 \times 10^6$ to $1 \times 10^7$ electrons m$^{-3}$ s$^{-1}$ are generated by cosmic rays and natural radiation due to atmospheric radioactivity. The electric field generated induces charges on the ground causing the acceleration of these electrons in the atmosphere (d). When these electrons collide with atmospheric atoms, knocking off electrons, they will form an electron-avalanche (e). Low-flux of high-energy (temperature) electrons will produce a low-intensity, blue-colored light ball (f), and high-flux of low-energy (temperature) electrons will produce a high-luminosity, red-colored light ball (g) in the opposite direction of the central white ball (h). Ejection of a small green light ball (i) from a white ball is due to radiation pressure produced by the interaction between very low frequency electromagnetic waves (j) and atmospheric ions in the central white-colored ball through ion-acoustic waves (IAW) (k). Centrifugal forces (l) caused by the rotation of the central white ball (m) can eject its hot and cold poles, forming, respectively, blue and red light balls.

IAW is a longitudinal oscillation of the ions (and the electrons) much like acoustic waves traveling in neutral gas. The IAW velocity will be (Alexeff & Neidigh, 1961):

$$V_{IAW} = \sqrt{\frac{\gamma_e Z_i k_B T_e + \gamma_i k_B T_i}{\langle m_i \rangle}} \quad (1)$$

where $k_B$ is Boltzmann's constant, $\langle m_i \rangle$ is the mean mass of the ion, $Z_i$ is its charge, $T_e$ is the temperature of the electrons, and $T_i$ is the temperature of the ions. Normally $\gamma_e$ is taken to be unity, on the grounds that the thermal conductivity of electrons is large enough to keep them isothermal on the time scale of ionic acoustic waves, and $\gamma_i$ is taken to be 3, corresponding to one-dimensional motion. In the plasma the electrons are often much hotter than the ions, in which case the second term in the numerator can be ignored. Thus, we have:

$$V_{IAW} \sim \sqrt{\frac{\gamma_e Z_i k_B T_e}{\langle m_i \rangle}} \quad (2)$$

According to Teodorani (2004), the HL spectrum gives a gas (ion) temperature of about $T_i$ = 5,000 K. Generally, the radiant species present in atmospheric plasma are $N_2$, $N_2^+$, $O_2$, and $O_2^+$, $NO^+$ (in dry air) and OH (in humid air). At higher temperatures, atomic emission lines of N and O, and (in the presence of water) H, are present (Laux, Spence, Kruger, & Zare, 2003). Thus, considering $T_e = 10 \times T_i = 50{,}000$ K, and mean ion mass as being:

$$\langle m_i \rangle = \frac{m_i(O^+) + m_i(N^+)}{2} \quad (3)$$

where $m_i(O^+) = 2.3 \times 10^{-16}$ kg is the ionic oxygen mass, and $m_i(N^+) = 2.6 \times 10^{-16}$ kg is the ionic nitrogen mass, we have $V_{IAW} \sim 10^4$ ms$^{-1}$. This is the velocity of the energetic wave packet of an ion acoustic wave in a dusty plasma. This value is close to the observed velocity of some ejected light balls from HL, which is estimated as being $2 \times 10^4$ $ms^{-1}$ (Teodorani, 2004).

Night vision systems revealed that the HL phenomenon produces a very strong infrared signature even when it is very faint or invisible in the optical range (Teodorani & Nobili, 2002). The dissociative recombination of $N_2^+$ in excited neutral atoms can explain the infrared emission by HL phenomenon even when it is very faint or invisible in the optical range. When VLF eject ions in high velocity from a white ball by IAW, dissociative recombination of $N_2^+$ [i.e. destroying molecular ions to produce excited neutral atomic species] can occur through the reaction $N_2^+ + e^- \rightarrow N + N$ + kinetic energy (Kasner, 1967). Dissociative recombination (DR) exhibits a high exothermicity, which makes DR the only source of kinetically energetic atoms (>1eV) (Peterson, Le Padellec, Danared, Dunn, Larsson, et al., 1998). These species (i.e. excited nitrogen atoms) are disconnected by IAW because they have zero charge. Few experimental studies of recombination have been carried out under conditions where dissociative recombination is the predominant process (Fowler & Atkinson, 1959). It will be the predominant electron loss process in the plasma only in regions where the concentration ratio of atomic to molecular ions is $>10^4$ (Biondi, 1969).

Why is the ejected ball always green-colored? Ejection of a small green light ball from HL is due to radiation pressure produced by the interaction between very low frequency electromagnetic waves (VLF) and atmospheric ions (present in the central white-colored ball) through ion-acoustic waves (IAW) (See Figure 1). Probably only $O_2^+$ ions (electronic transition ($b^4\Sigma_g^- \rightarrow a^4\Pi_u$)), with green emission lines, are predominantly transported by IAW. Electronic bands of $O_2^+$ ions occur in auroral spectra (Chamberlain, 1961, Nicolet & Dogniaux, 1950). Electron–molecular-ion dissociative recombination coefficient rate α as functions of electron temperature $T_e$ and cross sections $\sigma$ as a function of electron energy $E$ have been measured by Mehr and Biondi (1969) for $N_2^+$ and $O_2^+$ over the electron temperature interval 0.007 to 10 eV. The estimated temperature of HL is about 5,000 K (Teodorani, 2004). At this temperature, the rate coefficient of dissociative recombination will be, respectively, $\alpha(T_e)_{O2+} \sim 10^{-8}$ $cm^3$ $s^{-1}$, and $\alpha(T_e)_{N2+} \sim 10^{-7}$ $cm^3$ $s^{-1}$. Thus, the nitrogen ions will be decomposed in $N_2^+ + e^- \rightarrow N + N^*$ more rapidly than oxygen ions in the HL plasma. Only ionic-species are transported by IAW. Therefore, only oxygen ions will be predominantly ejected by IAW from a central white ball in HL phenomenon forming high-velocity green-light balls presenting a negative band of $O_2^+$ with electronic transition $b^4\Sigma_g^- \rightarrow a^4\Pi_u$. Additionally, the first positive bands of $N_2$($1PN_2$, electronic transition $B^3\Pi_g \rightarrow A^3\Sigma_u^+$) make a distinct contribution to the source spectrum of red balls, while the second positive band of $N_2$($2PN_2$, electronic transition $C^3\Pi_u \rightarrow B^3\Pi_g$) and the first negative band of $N_2^+$ ($1NN_2^+$, electronic transition $B^2\Sigma_u^+ \rightarrow X^2\Sigma_g^+$) play a minor role since they are caused by high-energy electrons—both bands are responsible for blue-colored balls around the central white ball in HL (Wescott, Sentman, Heavner, Hallinan, Hampton, & Osborne, 1996).

Relativistic runaway electron avalanche (RREA) is an avalanche growth of a population of relativistic electrons driven through a material (typically air) by an electric field. RREA has been hypothesized to be related to lightning initiation (Gurevich & Zybin, 2005), terrestrial gamma-ray flashes (Dwyer & Smith, 2005), and red sprites (Lehtinen, Bell, & Inan, 1999), and it is unique that it can occur at electric fields an order of magnitude lower than the dielectric strength of the material. When an electric field is applied to a material, free electrons will drift slowly through the material as described by electron mobility. For low-energy electrons, faster drift implies higher friction, so the drift speed tends to stabilize. For electrons with energy above about 1 keV, however, higher speeds imply lower friction. An electron with a sufficiently high energy, therefore, may be accelerated by an electric field to even higher and higher energies, encountering less and less friction as it accelerates. Such an electron is described as a "runaway." Free electrons with the density of $4 \times 10^6$ to $1 \times 10^7$ electrons $m^{-3}$ $s^{-1}$ are generated by cosmic rays and natural radiation due to atmospheric radioactivity (Paiva & Taft, 2011). The electric field generated by the rock fracture or stress induces charges on the ground that accelerate these electrons which ionize or excite $N_2$ and $O_2$ molecules in the air, forming the electron avalanche by RREA. Indentation fracture of moist andesite (under wet conditions) can produce a net negative charge density of about 0.6 C $m^{-3}$ $s^{-1}$. Typical occurrence altitude of the HL phenomenon is generally very low (a few tens of meters over the treetops), and the vast majority of the lights were reported to be below the tops of mountains (Bjorn, 2007). Mountainous soil has a mean dielectric constant (permittivity) $\varepsilon_s \sim 5$ (Saveskie, 2000). Thus, the electric potential in the air on the failure will be $\Delta V = q/4\pi\ \varepsilon_s\varepsilon_0 = 2.2$ GV. Let us calculate the electron number produced by the runaway electron avalanche (RREA) mechanism in HL phenomenon. The runaway electron avalanche multiplication factor is given by Dwyer (2003, 2007):

$$N_{RE} = \exp\left(\frac{\Delta V - 2.13\times10^6 I}{7.3\times10^6}\right) \tag{4}$$

where $\Delta V$ is the potential difference of the avalanche region in volts and $I$ is the column depth of the avalanche region in g/cm$^2$. In the case of HL altitude occurrence, atmospheric depth will be $I = 10^3$ g/cm$^2$ (Bacioiu, 2011). The number of electrons in the final path of the RREA avalanche will be $N_{RE}$ = exp (9.5) =

$10^4$ electrons. This value is $10^{12}$ times lower than that responsible for terrestrial gamma ray flashes in high altitudes on thunderclouds (Paiva, Pavão, & Bastos, 2009). Finally, high luminosity white balls around a central white ball are formed by a fragmentation process of Hessdalen lights–like dusty plasmas (Paiva & Taft, 2011). According to Teodorani (2004), sudden appearance of satellite light balls around a common nucleus can be related to the re-minimization of the effective surface energy (with the formation of new condensation nuclei) predicted by Turner's ball lightning model (Turner, 2003). However, several chemical species from rocks, such as scandium and silicon ions, were detected in the HL spectrum, suggesting dust from the valley (Bjorn, 2007). Thus, HL can sometimes assume the dusty plasma structure (Paiva & Taft, 2010). In this case, fragmentation of HL in a cluster of light balls can be produced by the interaction of low-frequency electromagnetic waves through the dust-acoustic waves. It is known that laboratory dusty plasmas are longitudinally fragmented by dust-acoustic waves (Barkan, Merlino, & D'Angelo, 1995). Similarly, video images show linear fragmentation of atmospheric light balls (UFO Hessdalen Norway, 2010, Amazing REAL looking UFO Sightings in INDIA, 2008). Dusty acoustic waves (DAW) is a complete analog to the common ionic-acoustic wave, where the dust particles take the role of the ions and ions and electrons take the role of the electrons (Thompson, Barkan, D'Angelo, & Merlino, 1997), and is an extremely low-velocity normal mode of a three-component dusty plasma comprising electrons, ions, and massive micrometer-size charged dust grains.

## Conclusion

The appearance of "satellite spheres," presenting different colors and intensities, composing a cluster around a main nuclear region, is produced by the interaction between high-energy electrons and very low frequency electromagnetic waves and atmospheric steady plasmas. A very strong infrared signature even when HL is very faint or invisible in the optical range is produced by the dissociative recombination of $N_2^+$ in excited neutral atoms (i.e. with high kinetic energy) in regions where the concentration ratio of atomic to molecular ions in the plasma is $>10^4$ (Biondi, 1969). Probably other related characteristics of HL can be explained by the high-energy electrons (accelerated by the RREA avalanche mechanism) accelerated in the atmosphere by electric fields from fractured rocks, or by the interaction between very low frequencies (from ground) and ions or charged dust particles in the atmospheric plasmas. Several chemical species from rocks, such as scandium and silicon ions, were detected in the HL spectrum (Bjorn, 2007) suggesting dust from the valley. Thus, HL can sometimes assume the dusty plasma structure (Paiva & Taft, 2010). The spectrum of the Hessdalen light phenomenon appears to be a continuum with no resolved lines (Teodorani, 2004). In the three-dimensional analysis of the intensity distribution of the lights, it appeared that the radiant power is due to a heated substance. Nevertheless, the light phenomenon, in both a photometric and spectroscopic sense, does not have the characteristics typical of a classic plasma of free electrons and ions (Teodorani & Nobili, 2002). When the atmospheric transparency was low, which was most of the time, and when the orbs were low over the horizon, the intensity distribution (ID) profile was very similar to that of an image of a heated, glowing plasma, i.e. a Gaussian shape with exponential wings. When the atmosphere was clear, with no fog, the ID profile of the image was nearly flat on top with steep sides such as when luminous point-like objects (e.g., stars) are observed through thick atmospheric layers. Probably this is due to the effect of optical thickness on the bremsstrahlung spectrum which is produced by electrons. At low frequencies, self-absorption modifies the spectrum to follow the Raleigh-Jeans part of the blackbody curve. This spectrum is typical of dense ionized gas. Additionally, the spectrum produced in the thermal bremsstrahlung process is flat up to a cutoff frequency, and falls off exponentially at higher frequencies. This sequence of events forms the typical spectrum of HL phenomenon when the atmosphere is clear, with no fog. One other possibility is that this typical spectrum is an effect due to solid particles (dust grains) immersed in a hot plasma. Unfortunately, the spectrum of laboratory dusty plasma still has not been obtained.

Finally, two stationary particles of the same electrical charge will repel each other, but two particles of the same electrical charge moving in parallel will develop a force of attraction. This can be the key to plasma confinement in nuclear fusion reactors. If atomic nuclei can be squeezed together by the positive charged mass flow, without the need for random collisions in superhot plasmas, then fusion engines could be designed to produce electricity directly by pulsing the fuel into the mass flow that compresses itself until fusion is reached. The extra energy from fusion will cause the mass flow to accelerate, and bind itself even tighter, releasing its energy as electromagnetic fields or energetic electrons until the fuel pulse is exhausted. In this way, the fusion ignition temperature could possibly be attained. Furthermore, helium lines have been detected in the HL spectrum (Bjorn, 2007). This can be strong evidence for cold nuclear fusion in these atmospheric plasmas since this chemical element is a product of nuclear fusion between deuterium atoms in nuclear fusion reactors. The currently accepted theory of special relativity (SRT) doesn't suggest that atomic nuclei can be squeezed together by positive charged mass flow. In SRT, mass velocities do not exceed light speed, so magnetic forces bringing nuclei together do not exceed Coulomb forces keeping them apart. If it nevertheless happens, that is exciting evidence that SRT is not entirely right. A number of other mechanisms can be suggested, without violating the

SRT principle. For example, quantum tunneling between deuterium nuclei can occur in HL phenomenon. In this process a particle passes through a potential barrier that it classically could not surmount. Winter is the season of Hessdalen Lights, when water is abundant. About one in every 6,000 water molecules contains deuterium atoms. On the other side, experiments on board the MIR orbital station (1991), the ISS (International Space Station) (2002), and the Kolibri-2000 satellite (2002) at an altitude of 400 km detected neutron bursts (one signature of nuclear fusion) in the equator regions connected with lightning discharges (Paiva, 2009). Whether these neutrons are thermonuclear in origin or are generated by photonuclear processes, this remains to be experimentally determined. In the case of HL, the mechanism responsible for helium emissions needs to be elucidated. Another possibility is that the helium comes from inside rocks. Fractured rocks can liberate helium ions which emit light when they recapture electrons in the atmosphere. In fact, there are rocks (for example, uraninite) that release helium from the natural decay of uranium.

## Acknowledgments

We acknowledge financial support from CNPq and Faperj (Brazil).

## References

Alexeff, I., & Neidigh, R. V. (1961). Observations of ion sound waves in plasmas. *Physical Review Letters, 7,* 223–225.

Amazing REAL looking UFO Sightings in INDIA Jan 26 2008 (2008/2011). http://www.youtube.com/watch?v=pSKu2tlgoRY&feature=related

Bacioiu, I. (2011). The theoretical interpretation of some cosmic rays reaching sea-level and the Meson Theory. *Romanian Reports in Physics, 63,* 161–171.

Barkan, A., Merlino, R. L., & D'Angelo, N. (1995). Laboratory observation of the dusty-acoustic wave mode. *Physics of Plasmas, 2,* 3563–3565.

Biondi, M. A. (1969). Atmospheric electron–ion and ion–ion recombination processes. *Canadian Journal of Chemistry, 47,* 1711–1719.

Bjorn, G. H. (2007). Optical Spectrum Analysis of the Hessdalen Phenomenon. Preliminary Report. pp. 1–12.

Chamberlain, J. W. (1961). *Physics of the Aurora and Air-Glow*. New York: Academic Press.

Dwyer, J. R. (2003). A fundamental limit on electric fields in air. *Geophysical Research Letters, 30,* 2055.

Dwyer, J. R. (2007). Relativistic breakdown in planetary atmospheres. *Physics of Plasmas, 14,* 042901-042901-17.

Dwyer, J. R., & Smith, D. M. (2005). A comparison between Monte Carlo simulations of runaway breakdown and terrestrial gamma-ray flash observations. *Geophysical Research Letters, 32,* L22804.

Enomoto, Y., & Hashimoto, H. (1990). Emission of charged particles from indentation fracture of rocks. *Nature, 346,* 641.

Fowler, R. G., & Atkinson, W. R. (1959). Electron recombination in atomic hydrogen. *Phvsical Review, 113,* 1268.

Gurevich, A. V., & Zybin, K. P. (2005). Runaway breakdown and the mysteries of lightning. *Physics Today, 58*(5), 37.

Kasner, W. H. (1967). Study of the temperature dependence of electron–ion recombination in nitrogen. *Physical Review, 164,* 194.

Laux, C. O., Spence, T. G., Kruger, C. H., & Zare, R. N. (2003). Optical diagnostics of atmospheric pressure air plasmas. *Plasma Sources Science and Technology, 12*, 125.

Lehtinen, N. G., Bell, T. F., & Inan, U. S. (1999). Monte Carlo simulation of runaway MeV electron breakdown with application to red sprites and terrestrial gamma ray flashes. *Journal of Geophysical Research, 104*(A11), 24699–24712.

Leone, M. (2003). A Rebuttal of the EMBLA 2002 Report on the Optical Survey in Hessdalen*.* pp. 1–27. Italian Committee for Project Hessdalen. http://www.itacomm.net/ph/rebuttal.pdf

Lockner, D. A., Johnston, M. J. S., & Byerlee, J. D. (1983). A mechanism to explain the generation of earthquake lights. *Nature, 302,* 28–33.

Mehr, F. J., & Biondi, M. A. (1969). Electron temperature dependence of recombination $O_2^+$ and $N_2^+$ ions with electrons. *Physical Review, 181,* 264–71.

Nicolet, M., & Dogniaux, R. (1950). Nouvelles suggestions au sujet de l'interpretation du spectre des aurores. *Journal of Geophysical Research, 55,* 21.

Ogawa, T., Oike, K., & Miura, T. (1985). Electromagnetic radiations from rocks. *Journal of Geophysical Research, 90,* 6245.

Paiva, G. S. (2009). Terrestrial gamma-ray flashes caused by neutron bursts above thunderclouds. *Journal of Applied Physics, 105,* 083301-083301-4.

Paiva, G. S., Pavão, A. C., & Bastos, C. C. (2009). "Seed" electrons from muon decay for the runaway mechanism in the terrestrial gamma ray flash production. *Journal of Geophysical Research, 114*(D13), 3205.

Paiva, G. S., Pavão, A. C., Vasconcelos, E. A., Mendes, O. Jr., & Silva, Jr., E. F. (2007). Production of ball-lightning–like luminous balls by electrical discharges in silicon. *Physical Review Letters, 98,* 048501-1.

Paiva, G. S., & Taft, C. A. (2010). A hypothetical dusty-plasma mechanism of Hessdalen lights. *Journal of Atmospheric and Solar-Terrestrial Physics, 72,* 1200–1203.

Paiva, G. S., & Taft, C. A (2011). Hessdalen lights and piezoelectricity from rock strain. *Journal of Scientific Exploration, 25,* 273–279.

Park, S. K., Johnson, M. J. S., Madden, T. R., Morgan, F. D., & Morrison, H. F. (1993). Electromagnetic precursors to earthquakes in the ULF band: A review of observations and mechanisms. *Reviews of Geophysics, 31,* 117.

Pasko, V. P., & George, J. J. (2002). Three-dimensional modeling of blue jets and blue starters. *Journal of Geophysical Research, 107,* 1458.

Pasko, V. P., Inan, U. S., & Bell, T. F. (2000). Fractal structure of sprites. *Geophysical Research Letters, 27,* 497–500.

Peterson, J. R., Le Padellec, A., Danared, H., Dunn, G. H., Larsson, M., Larson, A., Peverall, R., af Ugglas, M., & van der Zande, W. J. (1998). Dissociative recombination and excitation of $N_2^+$: Cross sections and product branching ratios. *Journal of Chemical Physics, 108,* 1979–1988.

Saveskie, P. N. (2000). Earth constants. *TAI Inc Consuletter International, 6*(5).

Serebryakova, O. N., Bilichenko, S. V., Chmyrev, V. M., Parrot, M., Rauch, J. L., Lefeuvre, F., & Pokhotelov, O. A. (1992). Electromagnetic ELF radiation from earthquake regions as observed by low-altitude satellites. *Geophysical Research Letters, 19,* 91.

Strand, E. (1990). Final Technical Report for Project Hessdalen—Part I (1984). 2nd International Symposium on Ball Lightning, June 26–28 1990, Budapest.

Takaki, S., & Ikeya, M. A. (1998). Dark discharge model of earthquake lightning. *Japanese Journal of Applied Physics, 37,* 5016–5020.

Teodorani, M. A. (2004). Long-term **s**cientific survey of the Hessdalen phenomenon. *Journal of Scientific Exploration, 18,* 217−251.

Teodorani M., & Nobili, G. (2002). EMBLA2002: Optical and Ground Survey in Hessdalen. Project

Hessdalen Articles and Reports. http://hessdalen.hiof.no/reports/EMBLA_2002_2.pdf

Thompson C., Barkan, A., D'Angelo, N., & Merlino, R. L. (1997). Dust acoustic waves in a direct current glow discharge. *Physics of Plasmas, 4,* 2331.

Turner, D. J. (2003). The missing science of ball lightning. *Journal of Scientific Exploration, 17,* 435–496.

UFO Hessdalen Norway (2010). http://www.youtube.com/watch?v=fSgPBOBSJrI

Wescott, E. M., Sentman, D. D., Heavner, M. J., Hallinan, T. J., Hampton, D. L, & Osborne, D. L. (1996). The optical spectrum of aircraft St. Elmo's fire. *Geophysical Research Letters, 23,* 3687–3690.